A Density Functional Theory Study of the Structure and Energetics of Zincate Complexes

Grant D. Smith,* Richard Bell, and Oleg Borodin

Department of Materials Science and Engineering and Department of Chemical and Fuels Engineering, 122 South Central Campus Drive, Rm. 304, University of Utah, Salt Lake City, Utah 84112

Richard L. Jaffe

NASA Ames Research Center, Moffett Field, California 94035

Received: January 7, 2001; In Final Form: March 27, 2001

We have conducted a density functional theory (DFT) investigation of zincate species. The accuracy of the DFT/B3LYP method and the adequacy of the atomic basis sets employed were established through investigation of the ionization potentials of Zn, the geometry and bond energy of ZnO, and the geometries and energies of selected Zn−OH and Zn−H_2O complexes. Our investigation revealed that the $[Zn(OH)]^+$, $Zn(OH)_2$, and $[Zn(OH)_3]^-$ zincate complexes are stable in the gas phase. However, we found that dissociated $[Zn(OH)_3]^-$ + OH^- is more stable than $[Zn(OH)_4]^{2-}$ in the gas phase and that the gas-phase geometry of $[Zn(OH)_4]^{2-}$ differs significantly from that gleaned from experimental studies of aqueous KOH/zincate solutions. We also investigated zincate complexes involving molecular water and K^+ cations in order to better understand the influence of condensed phase effects in aqueous KOH solutions on the stability and geometry of the zincate complexes. We found that water does not significantly influence complex binding energies or the geometries of the underlying $[Zn(OH)_n]^{2-n}$ complexes for $n = 1$, 2, and 3. In contrast, for $[Zn(OH)_4]^{2-}$ the introduction of water strongly stabilizes the complex relative to the gas phase and results in a structure close to that observed experimentally. We were unable to find a stable $[Zn(OH)_4(H_2O)_2]^{2-}$ complex with a planar $Zn(OH)_4$ arrangement and close Zn−H_2O coordination, corresponding to a Zn−O coordination of number of six, as has been suggested in some interpretations of experiments. We found through investigation of the $K_2Zn(OH)_4$ complex that K^+ cations are also effective in engendering a structure that is very close to experiment and that K^+ ions are even more strongly bound to the $[Zn(OH)_4]^{2-}$ complex than water. Finally, we determined the structure and stability of $[ZnO(OH)_2]^{2-}$(oxodihydroxozincate), a species that has been hypothesized to be important in water-poor zincates solutions.

I. Background and Motivation

The primary electrochemical components of an alkaline battery are a zinc anode and a transition metal oxide (XO_2) cathode combined with aqueous KOH as the electrolyte.[1,2] Anodic oxidation of the zinc electrode in concentrated KOH solution produces Zn(II) ions resulting in the formation of zincates, e.g., $[Zn(OH^-)_n(H_2O)_m]^{(2-n)}$ complexes. During battery discharge the electrolyte typically becomes supersaturated in Zn^{2+} relative to the ZnO precipitate, which is the final zinc product of the electrochemical discharge reaction[3,4]

$$Zn + H_2O + 2XO_2 \rightarrow ZnO + 2XOOH \qquad (1)$$

Optimal battery operation depends on controlling the electrochemical performance of the electrolyte, including the degree of supersaturation of the zincate solutions. For this reason many experimental investigations have been performed in order to identify the structure of zincate species formed during battery discharge and the mechanism(s) responsible for formation of the ZnO precipitate. It is generally believed that the predominant zincate species in concentrated KOH electrolyte solutions is $[Zn(OH_4)]^{2-}$ or tetrahydroxozincate (TZT), formed by the half-cell reaction[2]

$$Zn + 4OH^- \rightarrow [Zn(OH)_4]^{2-} + 2e^- \qquad (2)$$

The presence of TZT has been confirmed by potentiometric measurements,[5] polarization measurements,[6] proton NMR measurements,[7−10] Raman and infrared spectroscopy,[7,11−13] and EXAFS.[14] On the basis of ^{67}Zn NMR,[15] neutron diffraction,[15] and EXAFS[16] studies it has been proposed that the general formula for the zincate ion is $[Zn(OH)_4(H_2O)_2]^{2-}$, where two H_2O molecules are positioned along the axis perpendicular to the $[Zn(OH)_4]^{2-}$ plane.[16] More recently, the species $[Zn(OH)_4(H_2O)_2]^{2-}$ has come under scrutiny. The existence of this structure was refuted in a multiple-scattering EXAFS investigation used to determine the structure of the complex ion in undersaturated solutions.[14] The authors[14] argued that the only zincate species present was tetrahedrally coordinated $[Zn(OH)_4]^{2-}$.

Supersaturation occurs when Zn(II) is present in solution in concentrations greater than the solubility limit of ZnO. It was once proposed that colloidal Zn^{2+} is responsible for supersaturation, but subsequent light scattering measurements have disproved this hypothesis.[17,18] Since the concentration of $[Zn(OH)_4]^{2-}$ appears to saturate when the solubility limit of ZnO is reached,[10] the existence of additional zincate species such as $Zn(OH)_2(H_2O)_2$ and $[Zn(OH)_3(H_2O)]^-$ has been postulated[7,19,20] in order to account for supersaturation. The proposed decomposition reactions for these species are

* Author to whom correspondence should be addressed.

10.1021/jp0100710 CCC: $20.00
Published on Web 06/12/2001

$$[Zn(OH)_2(H_2O)_2] \rightarrow ZnO + 3H_2O \quad (3)$$

$$[Zn(OH)_3(H_2O)]^- \rightarrow ZnO + OH^- + 2H_2O \quad (4)$$

Other studies concluded that these di- and trihydroxozincates cannot be present because their decomposition reactions 3 and 4 are not consistent with the observed ratio of precipitated ZnO to released OH^- of 1:2.[21] As a result, three other mechanisms for ZnO precipitation and corresponding zincate intermediates consistent with this ratio have been proposed.[21] The first mechanism begins with the reaction

$$[Zn(OH)_4]^{2-} \rightarrow [ZnO(OH)_2]^{2-} + H_2O \quad (5)$$

forming oxodihydroxozincate (ODHZ). Association of two ODHZ could form a complex that leads to the production of 2ZnO and $4OH^-$. The second mechanism proposes the formation of a zincate polymer initiated by the reaction

$$2[Zn(OH)_4]^{2-} \rightarrow [(OH)_3Zn-O-Zn(OH)_3]^{4-} + H_2O \quad (6)$$

Decomposition follows from the combination of two dimeric species

$$2[(OH)_3Zn-O-Zn(OH)_3]^{4-} \rightarrow 4ZnO + 8OH^- + 2H_2O \quad (7)$$

This mechanism has also been proposed elsewhere.[18] The third mechanism is the dimerization of $[Zn(OH)_4(H_2O)_2]^{2-}$. The proposed reaction leading to the formation of ZnO is

$$2[Zn_2(OH)_8(H_2O)_3]^{4-} \rightarrow 4ZnO + 8OH^- + 10H_2O \quad (8)$$

In recent EXAFS studies of saturated zincate solutions,[14] no evidence has been found to support the existence of the zincate species $Zn(OH)_2(H_2O)_2$, $[Zn(OH)_3(H_2O)]^-$, or the polymeric species proposed in reactions 6−8. A ^{67}Zn NMR and EXAFS study[10] of supersaturated zincate solutions also failed to find evidence of polymeric zincate species, leading the authors to support ODHZ as a likely species to account for supersaturation.[10]

In this work we employ density functional theory (DFT) quantum chemistry methods to investigate the structures and energies of a number of proposed zincate complexes. DFT methods have proven reliable for investigating gas-phase molecular properties, but despite recent progress in methodology and computational hardware remain too computationally demanding to be used for solutions as complex as zincates. The intent of this work to determine which zincate species are likely to form in the electrolyte solutions of interest by performing DFT studies of likely complexes using reasonable basis sets. We investigate the manner in which hydroxide groups are arranged around a Zn^{2+} ion or ZnO moiety, determine the stability of gas-phase complexes, and explore the role that water and K^+ cations may play in influencing zincate structures in solution.

II. Methodology

All ab initio molecular orbital calculations were carried out on 433 Dec Alpha workstations at the University of Utah and on NASA Ames IBM RS6000 workstations using the Gaussian98 suite of quantum chemistry programs.[22]

A. Basis Sets. Correlation consistent basis sets, labeled aug-cc-pVTZ,[23] were chosen for both O and H, and a polarized split-valance basis set 6-311+G(2df) was selected for Zn^{2+}. The aug-cc-pVTZ basis set for O is (10s,5p,2d,1f) contracted to [4s,3p,2d,1f] with diffuse (s, p, d, f) basis functions added. For H, the basis set is (5s,2p,1d) contracted to [3s,2p,1d] with diffuse (s, p, d) basis functions added. The 6-311+G(2df) basis set for Zn is (15s,11p,6d,2f,1g) contracted to [10s,7p,4d,2f,1g] and is an unpublished hybrid basis created by Gaussian and included in the Gaussian98 programs. The exponents and coefficients for this basis set are given in Table 1. For zincate complexes where K^+ has been included as a counterion, we used the core valence double-ζ potassium basis set[24] consisting of (15s,12p,-2d) contracted to [6s,5p,2d].

B. Validation of Basis Sets and Level of Theory. *Relativistic Effects.* We tested the adequacy of the DFT approach using the B3LYP[25,26] functional with our selected basis sets by carrying out calculations of Zn ionization potentials (IP) as well as ZnO ground electronic state bond length (R_e) and dissociation energy (D_e). To determine the magnitude of relativistic effects in these calculations, we compared the all electron calculations with results of relativistic and nonrelativistic effective core potential (RECP and ECP, respectively) calculations using the SDD potentials and basis sets for zinc.[27] The ECP and RECP parameters and contracted Gaussian basis sets were derived to simultaneously reproduce the valence orbitals and energies from Hartree−Fock calculations for the low-lying electronic states of Zn and Zn^+. For the entire first transition metal series, the resulting IP and atomic and ionic excitation energies differ by only 0.1 eV from comparable all electron Hartree−Fock calculations. For zinc, the agreement between CISD+Q/RECP calculations and experimental data for the IP and excitation energies is ∼0.3 eV. The SDD potentials we used in the present study replace a neon core so transition metal core−valence correlation effects due to the 3s and 3p electrons can be treated in this framework. The SDD basis set consists of (8s,7p,6d) contracted to [6s,5p,3d] to which we added the two f-functions from the all-electron zinc basis set (denoted SDD+2f with f exponents 3.24 and 0.81). Our DFT results were also compared with MP2, QCISD(T) and CCSD(T) ab initio calculations, representing increasingly better treatment of electron correlation.

Zn and ZnO. The calculated IP for Zn and Zn^+ and R_e and D_e for ZnO are given in Table 2. It can be seen that inclusion of relativistic effects increases the Zn and Zn^+ IP by 0.2 and 0.3 eV, respectively, but slightly decreases the ZnO D_e and has almost no influence on R_e. The QCISD(T)/RECP results are within 0.1 eV of experiment[28] for both ionization potentials and 3 kcal/mol for ZnO D_e. Unfortunately, the Gaussian98 ECP implementation cannot be used to compute analytic force constants and vibration frequencies for basis sets containing f-functions, so this level calculation could not be used in the present study of zincate complexes. In Table 2 it can also be seen that both the B3LYP and MP2 results for ZnO D_e differ from the QCISD(T) result by about 10 kcal/mol. The QCISD-(T) value is in good agreement with experiment,[29] with the B3LYP method underestimating the bond energy and the MP2 method overestimating it. However, the B3LYP R_e is in excellent agreement with the QCISD(T) value, while the MP2 calculations result in a 0.04 Å smaller bond length.

Zn−OH and Zn−H_2O Complexes. The influence of the level theory on the geometries and energies of $[Zn(OH)]^+$ and $[Zn(H_2O)]^{2+}$ complexes was also investigated. Results are presented in Table 3. Here, the B3LYP and MP2 methods give similar results for bond length and angles, but the B3LYP calculations overestimate the Zn^{2+}−ligand binding energy by 14 kcal/mol for hydroxide and 6 kcal/mol for water compared to QCISD-(T) values. However, for $Zn(OH)_2$, the energy gained in adding

TABLE 1: Zinc 6-311+G(2df) Basis Set

S	exp	coeff	P	exp	coeff	D	exp	coeff	F	exp	coeff	G	exp	coeff
1	316336.	0.0003200	1	2213.18	0.00262	1	58.4084	0.02759	1	3.24	1.0	1	1.62	1.0
	48561.0	0.0024200		527.050	0.02091		16.4492	0.14994	2	0.81	1.0			
	11157.4	0.012410		172.293	0.09501		5.57570	0.36929						
	3205.01	0.048640		66.0814	0.26855	2	1.88441	1.0						
	1068.58	0.14807		27.6863	0.43542	3	0.572305	1.0						
	396.394	0.32526	2	12.1841	1.0	4	0.162	1.0						
2	159.806	1.0	3	4.98796	1.0									
3	68.5890	1.0	4	2.05791	1.0									
4	23.7081	1.0	5	0.798609	1.0									
5	10.0372	1.0	6	0.162455	1.0									
6	2.81043	1.0	7	0.047769	1.0									
7	1.6964	1.0												
8	0.146951	1.0												
9	0.0511420	1.0												
10	0.0153430	1.0												

TABLE 2: Influence of the Level of Theory on Zn and ZnO Properties

method[a]	Zn IP (eV)	Zn^+ IP (eV)	ZnO R_e (Å)	ZnO D_e (kcal/mol)
B3LYP	9.43	18.38	1.71	−29.8
MP2	8.92	17.54	1.68	−51.5
QCISD(T)	9.11	17.51	1.72	−39.2
B3LYP/RECP	9.62	18.72	1.70	−27.3
MP2/RECP	9.12	17.90	1.66	−50.9
QCISD(T)/RECP	9.30	17.89	1.71	−35.5
MP2/ECP	8.92	17.57	1.67	−53.0
QCISD(T)/ECP	9.11	17.56		
CCSD(T)[b]			1.72	−38.7
QCISD(T)/BS[c]			1.73	−31.0
experiment	9.39[d]	17.96[d]		−38.3[e]

[a] All electron calculations utilized Zn 6-311+G(2df) and O aug-cc-pVTZ basis sets. RECP and ECP calculations utilized a Zn SDD+2f basis set and the same O basis set. [b] Ref. 30. [c] Ref. 31. [d] Ref. 28. [e] Ref. 29.

TABLE 3: Geometry and Binding Energy for $[Zn(OH)]^+$ and $[Zn(H_2O)]^{2+}$ Complexes

$[Zn(OH)]^+$

method[a]	R (Zn−O) (Å)	R (O−H) (Å)	Zn−O−H angle	BE[b] (kcal/mol)
B3LYP	1.76	0.97	113.8	−437.9
MP2	1.74	0.97	113.7	−423.8
CCSD(T)[c]				−424.7
QCISD(T)[c]				−424.8

$[Zn(H_2O)]^{2+}$

method[a]	R (Zn−O) (Å)	R (O−H) (Å)	H−O−H angle	BE[b] (kcal/mol)
B3LYP	1.87	0.98	108.2	−104.2
MP2	1.85	0.98	109.6	−97.9
CCSD(T)[c]				−97.3

[a] All electron calculations utilized Zn 6-311+G(2df) and O, H aug-cc-pVTZ basis sets. [b] Binding energy relative to Zn^{2+} and OH^- or H_2O. [c] Energy computed at the MP2 geometry.

the second OH^- ligand is −254.3 kcal/mol at the B3LYP level as compared to −251.8 kcal/mol at the HF level, −255.8 kcal/mol at the MP2 level, and −255.2 kcal/mol at the QCISD(T) level. Encouragingly, the large dependence of ligand binding energy on the level of quantum chemistry calculation appears to hold only for the first (most strongly bound) ligand, with the sequential binding energy for the second hydroxide ligand being much less sensitive to the level of theory.

Our investigation of the influence of basis set and level of theory for structures and energies of Zn, ZnO, and Zn−OH and Zn−H_2O complexes reveals that (1) relativistic effects are not large in these systems, (2) our QCISD(T) results are in good agreement with the larger basis set CCSD(T) calculations of Bauschlicher and Partridge,[30] and are an improvement over the 6-311+G(d) basis used by Boldyrev and Simon,[31] (3) the B3LYP geometries are in excellent agreement with QCISD(T) results, and (4) the B3LYP method with our selected basis sets yields an accurate value (compared to higher level of theory) for the sequential binding energy for $Zn(OH)_2$. On the basis of these observations, we believe our basis sets and the use of the B3LYP method represent a practical compromise between computational efficiency and accuracy for the larger zincate structures considered in this study.

C. Partial Charge Determination. To determine the effective partial charge on each atom for all zincate complexes, we employed the electrostatic potential (EP) charge method using the ChelpG algorithm.[32]

III. Geometries and Energies of $[Zn(OH)_n]^{(2-n)}$ Complexes

A. Geometries. To ensure that no important complex geometries were overlooked, all structures were optimized first at the restricted Hartree−Fock (SCF) level where each structure was initially given C_1 symmetry using the basis sets described above. From the results of these geometry optimizations, the symmetry point group for the optimized structure of each complex was identified. Restricting each complex to that point group, a second optimization was performed at the B3LYP level.[33] The optimized structure of hydroxide is shown in Figure 1a.

$[Zn(OH)]^+$. The B3LYP optimized structure for the $[Zn(OH)]^+$ species is illustrated in Figure 1b. Considering only electrostatic forces, the Zn−O−H moiety should exhibit a linear geometry. However, the OH^- group rotates to form a dative bond using the filled 1π orbital of OH^- and the empty Zn 4s orbital, resulting in C_s symmetry. Dative bonding allows for charge to be transferred to Zn dramatically reducing the EP charge on Zn, as shown in Table 4.

$Zn(OH)_2$. The $Zn(OH)_2$ complex has C_2 symmetry as shown in Figure 1c. There are minimal ligand field effects because of the filled Zn 3d shell, so the hydroxide ligands are free to take positions that minimize their electrostatic repulsion. Consequently the O−Zn−O angle is nearly linear. By taking positions on opposite sides of Zn and bending away from a linear geometry, the 1π orbitals of the OH^- ligands form dative bonds with the spherically symmetrical Zn 4s orbital. The combination of electrostatic repulsion and dative bonding leads to two hydroxide ligands that are structurally similar to the single ligand

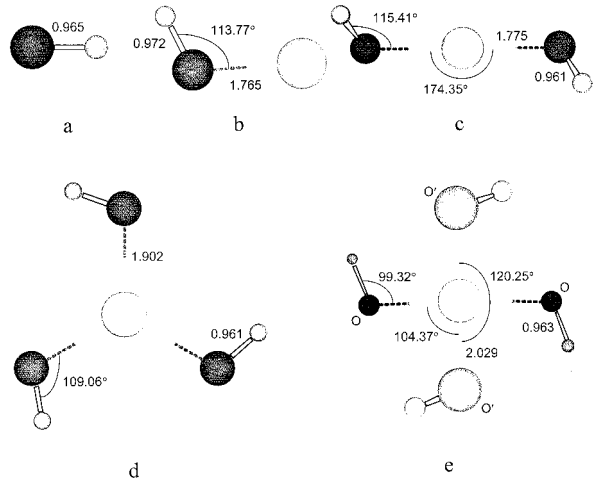

Figure 1. B3LYP optimized geometries of the hydroxide ion and $[Zn(OH)_n]^{2-n}$ zincate species. Selected bond lengths (Å) and valence angles are shown.

TABLE 4: The Zn Charge in Zincate Complexes from Electrostatic Potential Calculations

zincate complex	Zn EP charge (electron charge)
Zn^{2+}	2.00
$[Zn(OH)]^+$	1.24
$Zn(OH)_2$	0.77
$[Zn(OH)_3]^-$	0.88
$[Zn(OH)_4]^{2-}$	1.51
$[Zn(OH)(H_2O)]^+$	0.97
$[Zn(OH)(H_2O)_3]^+$	0.66
$Zn(OH)_2(H_2O)_2$	0.69
$[Zn(OH)_3(H_2O)]^-$	0.77
$[Zn(OH)_4(H_2O)_2]^{2-}$	1.31
$K_2Zn(OH)_4$	1.16
$[ZnO(OH)_2]^{2-}$	0.82

in $[Zn(OH)]^+$, as shown in Figure 1b. The H−O−O−H torsion angle is 96.37°, similar to the hydrogen peroxide structure. Table 4 shows that the EP charge on the zinc atom is further reduced due to electron donation to the Zn 4s orbital by the hydroxide ligands.

$[Zn(OH)_3]^-$. The point group symmetry for $[Zn(OH)_3]^-$, displayed in Figure 1d, is C_{3h}. The Zn−O bond distance is larger than in $[Zn(OH)]^+$ and $Zn(OH)_2$ due to electrostatic repulsion between ligands. However, the hydroxide ligands are sufficiently close that attractive H···O interactions stabilize the planar pinwheel structure of $[Zn(OH)_3]^-$ and result in a smaller Zn−O−H angle than seen in the single and double ligand complexes.

$[Zn(OH)_4]^{2-}$. The addition of a fourth hydroxide ligand produces tetrahydroxozincate (TZT). Crowding is significant as four OH^- ligands compete for space around the central Zn atom, and the electrostatic repulsion between neighboring ligands is significantly larger than in the other zincate species, Consequently, the Zn−O bond lengths are significantly greater, as shown Figure 1e. The larger Zn−O distance reduces the overlap of the 1π orbital of each OH^- group with the Zn 4s orbital resulting in much less charge donation to Zn, as shown in Table 4. The ZnO_4 subunit prefers to have T_d point group symmetry in order to minimize electrostatic repulsion between ligands. However, the OH^- ligands bend away from a linear Zn−O−H orientation to allow the 1π orbitals of the ligands to form dative bonds with the empty Zn 4s orbital and to maximize H···O attraction between ligands, producing a distorted tetrahedron with the S_4 symmetry shown in Figure 1e. Four of the six O−Zn−O bond angles have a value of 104.37° and the other two are 120.25°. The two larger O−Zn−O bond angles, denoted O−Zn−O and O′−Zn−O′ in Figure 1e, correspond to ligand pairs that do not experience significant H···O attraction. The four smaller bond angles, denoted O−Zn−O′ in Figure 1e, correspond to ligand pairs that are so stabilized. The H···O attraction between neighboring ligands is also responsible for decreasing the Zn−O−H angle compared to the other complexes.

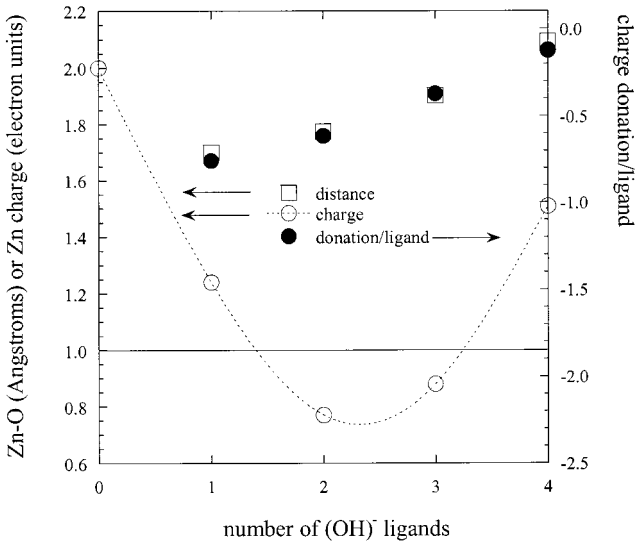

Figure 2. Zn electrostatic potential charge, Zn−O distances for hydroxide ligands, and charge donatation per ligand for $[Zn(OH)_n]^{2-n}$ as a function of n. The dashed line serves to guide the eye. The solid line at $q_{Zn} = 1$ illustrates the relatively constant value of Zn charge after addition of the first ligand.

B. Zn Electrostatic Charge. Figure 2 reveals a complex dependence of the Zn electrostatic charge, as determined from electrostatic potential calculations, on the number of hydroxide ligands. The charge donation to Zn per ligand, q_d, determined from the relationship

$$q_d = (q_{Zn} - 2)/n \tag{9}$$

where q_{Zn} is the Zn charge and n is the number of ligands, is clearly correlated with the Zn−O distance, as shown in Figure 2. With increasing Zn−O distance, dative bonding between the hydroxide ligand and Zn is reduced, resulting in a reduction in charge donation per ligand.

C. Binding Energies. The gas-phase binding energies for the reactions

$$Zn^{2+} + nOH^- \rightarrow [Zn(OH)_n]^{2-n} \tag{10}$$

and the sequential binding energies for the reactions

$$OH^- + [Zn(OH)_{(n-1)}]^{(3-n)} \rightarrow [Zn(OH)_n]^{2-n} \tag{11}$$

are given in Table 5. Note that the total binding energy for $[Zn(OH)_4]^{2-}$ is less than that of $[Zn(OH)_3]^-$, yielding a positive sequential binding energy for $[Zn(OH)_4]^{2-}$. This implies that $[Zn(OH)_4]^{2-}$ is unstable in the gas phase, rejecting a hydroxide ligand in favor of forming the more stable $[Zn(OH)_3]^- + OH^-$. The underlying reason for the lower stability of $[Zn(OH)_4]^{2-}$ is the considerably larger ligand−ligand repulsion energy for TZT compared to $[Zn(OH)_3]^-$ (the ligand−ligand energies are also given in Table 5). If the ligand−ligand repulsion energies are

TABLE 5: Ligand Binding Energies for Zincate Complexes (kcal/mol)

complex	TBE[a]	SBE[b]	L−L R. E.[c]
$[Zn(OH)]^+$ (C_s)	−437.90	−437.90	0.00
$Zn(OH)_2$ (C_2)	−692.19	−254.29	90.37
$[Zn(OH)_3]^-$ (C_{3h})	−758.52	−66.35	260.82
$[Zn(OH)_4]^{2-}$ (S_4)	−707.51	51.02	480.09

[a] Total ligand binding energy, $E\{[Zn(OH)_n]^{(2-n)}\} - E\{Zn^{2+}\} - nE\{OH^-\}$. [b] Sequential ligand binding energy, $E\{[Zn(OH)_{n-1}]^{(2-n)}\} - E\{[Zn(OH)_{n-1}]^{(3-n)}\} - E\{OH^-\}$. [c] Ligand−ligand interaction (repulsion) energy, determined from single point quantum chemistry calculations of the ligands in a configuration corresponding to that for the zincate complex, but performed in the absence of the zinc.

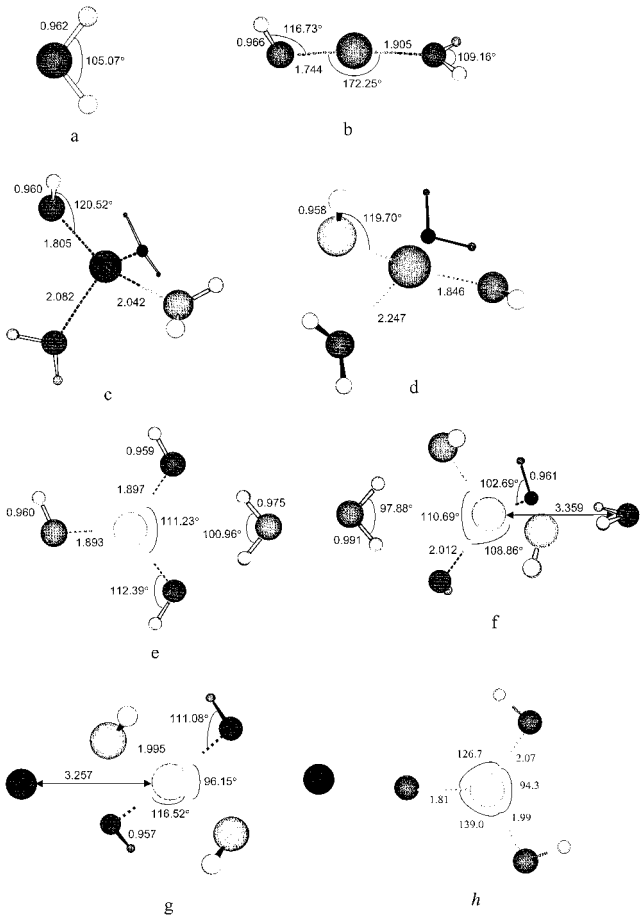

Figure 3. B3LYP optimized geometries of water and $[Zn(OH)_n(H_2O)_m]^{2-n}$ zincate species. Selected bond lengths (Å) and valence angles are shown. Also shown are the optimized $K_2Zn(OH)_4$ and $[ZnO(OH)_2]^{2-}$ (ODHZ) structures.

removed from the sequential binding energies all zincate complexes would be stable in the gas phase.

IV. Geometries and Energies of $[Zn(OH)_n(H_2O)_m]^{(2-n)}$ Complexes

A. Geometries. The same procedure described above for zincate complexes without water was employed in exploration of hydrated complexes.[33] The B3LYP optimized geometry for water is shown in Figure 3a.

$[Zn(OH)(H_2O)]^+$. The $[Zn(OH)(H_2O)]^+$ complex, with C_s point group symmetry, is illustrated in Figure 3b. The presence of a single water molecule does not significantly alter the geometry of the $Zn(OH)^+$ moiety from the isolated case (see Figure 1b). The Zn−O bond distance is shortened slightly and the Zn−O−H bond angle is opened slightly. The Zn−O distance for the water ligand is 0.16 Å larger than for the hydroxide ligand. As is the case with $Zn(OH)_2$, the electrostatic repulsion between the ligands is minimized when they are positioned on opposite sides of Zn, yielding an O−Zn−O angle similar to that observed for $Zn(OH)_2$ (see Figure 1c). In comparing the Zn charges for $[Zn(OH)(H_2O)]^+$ and $Zn(OH)_2$ in Table 4, we note that less charge is transferred to Zn for $[Zn(OH)(H_2O)]^+$ consistent with the larger Zn−O distance for the water ligand.

$[Zn(OH)(H_2O)_3]^+$. The zincate complex $[Zn(OH)(H_2O)_3]^+$ has C_s symmetry as illustrated in Figure 3c. Hydrogen bonding effects play a role in determining this molecular configuration, which exhibits a near tetrahedral ZnO_4 structure. This near tetrahedral geometry indicates that electrostatic repulsion effects are relatively unimportant in determining the geometry of $[Zn(OH)(H_2O)_3]^+$ compared to the corresponding four hydroxide ligand complex $[Zn(OH)_4]^{2-}$ (Figure 1e). The presence of three water molecules has a significant influence on the structure the Zn(OH) moiety. Two water molecules are positioned such that one O−H bond of each water is nearly parallel to the Zn−O bond of the OH ligand. For the hydroxide ligand, the Zn−O bond distance is increased significantly compared to $[Zn(OH)]^+$ and the Zn−O−H bond angle is somewhat opened. The Zn−O distances for each water ligand are longer than the Zn−O bond distance for the hydroxide ligand. However, the Zn−O distance for the hydroxide ligand is much shorter than that for the corresponding four hydroxide ligand structure (Figure 1e) and the Zn−O distances for the water ligands are comparable to the Zn−O distances for the hydroxide ligands in $[Zn(OH)_4]^{2-}$. Consequently, the total charge donation to Zn for $[Zn(OH)(H_2O)_3]^+$ is much larger than for $[Zn(OH)_4]^{2-}$, as can be seen in Table 4. As in the case with the single water complex, $[Zn(OH)(H_2O)]^+$, charge distribution in the Zn(OH) moiety of the $[Zn(OH)(H_2O)_3]^+$ complex resembles that of Zn^+-OH more closely than that of Zn^{2+}-OH^-.

$Zn(OH)_2(H_2O)_2$. The zincate structure shown in Figure 3d is that of $Zn(OH)_2(H_2O)_2$ with C_2 symmetry. Comparison with Figure 1c reveals how the water molecules alter the $Zn(OH)_2$ configuration. The water molecules are hydrogen bonded to the hydroxide ligands and are positioned on both sides of $Zn(OH)_2$, where one O−H bond from each water molecule is nearly parallel to the Zn−O bonds of the $Zn(OH)_2$ moiety. In the presence of two water ligands, the Zn−O bond lengths of $Zn(OH)_2$ are lengthened significantly, and the Zn−O−H bond angles are increased slightly. The addition of two water molecules decreases the H(O−Zn−O)H angle from 174.35° for isolated $Zn(OH)_2$ to 158.87° for the $Zn(OH)_2(H_2O)_2$ complex. However, unlike the $[Zn(OH)(H_2O)_3]^+$ complex the ZnO_4 arrangement in $Zn(OH)_2(H_2O)_2$ is far from tetrahedral, indicating the continued dominance of OH^-−OH^- electrostatic repulsion in determining the geometry of the complex. As the Zn−O distance for the hydroxide ligands is greater in $[Zn(OH)_2(H_2O)_2]$ compared to $Zn(OH)_2$, the smaller charge for Zn in the former indicates charge donation by the water molecules.

$[Zn(OH)_3(H_2O)_m]^-$. A stable geometry for tetrahedrally coordinated zincate complexes with three hydroxide and one water ligand could not be identified. In several attempts to prepare this complex from $[Zn(OH)_3(H_2O)_m]^-$ with $m = 1,2$ structures, the OH− ligands invariably formed a planar trigonal structure, similar to that found for $[Zn(OH)_3]^-$,with all the water hydrogen atoms hydrogen bonded to hydroxide oxygen atoms. The optimized structure of $[Zn(OH)_3(H_2O)]^-$ is shown in Figure 3e. The water is tilted slightly out of the ZnO_3 plane and the pinwheel structure observed for isolated $[Zn(OH)_3]^-$ is altered

to accommodate the water−hydroxide hydrogen bonding. That hydrogen bonding causes the O−Zn−O bond angle opening toward the water to decrease from 120° for isolated $[Zn(OH)_3]^-$ to 111.23°. The H−O−H water bond angle is also decreased from that found for the isolated water molecule. A slightly shorter Zn−O bond distance and a lower Zn EP charge (see Table 4) were found for $[Zn(OH)_3(H_2O)]^-$ compared to $[Zn(OH)_3]^-$.

$[Zn(OH)_4(H_2O)_2]^{2-}$. It has been suggested in the literature that $[Zn(OH)_4(H_2O)_2]^{2-}$ forms a planar $Zn(OH)_4$ subunit, analogous to $Zn(OH)_3$ (see Figure 1d), with the two waters in axial positions perpendicular to the $Zn(OH)_4$ plane.[16] Attempts to find a stable configuration for this complex resulted in the ZnO_4 moiety having S_4 symmetry with the water molecules pushed into a second solvation shell around Zn, as illustrated in Figure 3f. Calculation of the Hartree−Fock normal-mode vibration frequencies for planar $[Zn(OH)_4]^{2-}$ revealed an imaginary frequency corresponding to the out-of-the-plane rotation of the ligands. Hence the planar $[Zn(OH)_4]^{2-}$ complex is inherently unstable and will undergo a distortion to form a S_4 symmetry structure.

The lowest energy TZT−$(H_2O)_2$ complex, with two hydrogen-bonded water molecules straddling the O−Zn−O and ON−Zn−ON bond angles of $[Zn(OH)_4]^{2-}$ is shown in Figure 3f. The symmetry of this complex is S_4. The water molecules cause a decrease in the O−Zn−O and O′−Zn−O′ bond angles and an increase in the O−Zn−O′ bond angles bringing the ZnO_4 structure very close to T_d symmetry, which is consistent with the results of the recent solution phase EXAFS investigation.[14] The geometry of the water molecules is in turn influenced by TZT. The water bond angles are smaller, and the O−H bond lengths are longer. As with $[Zn(OH)_3(H_2O)]^-$ the reduction in the O−Zn−O bond angle is accompanied by a decrease in the Zn−O bond length. However, this value of 2.01 Å is still significantly greater than experimentally reported value of 1.96 ± 0.01 Å found in KOH solution.[14] Since the Zn−O bond distances are shortened with addition of two waters to TZT, more charge is donated to Zn reducing the EP charge on Zn, as shown in Table 4.

$K_2Zn(OH)_4$. In concentrated KOH solutions zincate species are likely to include counterions because there are insufficient water molecules present to completely hydrate all the ionic species. Figure 3g is an illustration of the charge neutral $K_2Zn(OH)_4$ complex. The two K^+ ions are located on opposite sides of TZT, where each K^+ ion bisects the O−Zn−O and O′−Zn−O′ bond angles. The electrostatic forces due to the positively charged K^+ ions affect the structure of TZT more than the hydrogen-bonded waters discussed above. The O−Zn−O and O′−Zn−O′ angles are reduced to 96.15°, and the O−Zn−O′ bond angles are increased to 116.52°. Moreover, the ligands are no longer hydrogen bonded in the manner observed for isolated TZT and hydrated TZT; each hydrogen is shared equally by two hydroxide ligands and points in the direction of a K^+ ion on the opposite side of TZT. The ZnO_4 subunit is nearer tetrahedral symmetry than for the isolated $[Zn(OH)_4]^{2-}$ complex, hence in better agreement with experiment,[7,14] but is less tetrahedral than the $[Zn(OH)_4(H_2O)_2]^{2-}$ complex. The K^+ ions shorten the Zn−O bond lengths to 1.995 Å, somewhat shorter than was found for $[Zn(OH)_4(H_2O)_2]^{2-}$ and closer to the experimental value of 1.96 ± 0.01 Å found in KOH solution.[14] In summary, the geometries of $[Zn(OH)_4(H_2O)_2]^{2-}$ and $K_2Zn(OH)_4$ complex are a consequence of the balancing of Zn−OH^- attraction (electrostatic and dative bonding), OH^-−OH^- interactions (electrostatic repulsion leading to a tetrahedral ZnO_4 arrangement, O···H attraction distorting this arrangement, reducing four O−Zn−O and opening up two O−Zn−O angles), and OH^-− H_2O or OH^-− K^+ attractions that close the two large O−Zn−O angles in order optimize OH^-− H_2O or OH^-− K^+ distances. This closing of two O−Zn−O angles results in an opening up of the remaining four, thereby reducing OH^-−OH^- electrostatic repulsion and allowing for shorter Zn−O bond lengths.

TABLE 6: Total Energy and Water Binding Energies (BE) for Hydrated Zincates and the Zincate Counterion Complexes

complex	energy (au)	water/counterion BE (kcal/mol)
$[Zn(H_2O)]^+$	−1854.963725	−104.22
$[Zn(OH)(H_2O)]^+$	−1931.423484	−57.57
$Zn(OH)_2(H_2O)_2$	−2084.068559	−18.27
$[Zn(OH)_3(H_2O)]^-$	−2083.539992	−15.53
$[Zn(OH)_4(H_2O)_2]^{2-}$	−2235.751886	−66.91
$[(OH)(H_2O)]^-$		−25.30
$[Zn(OH)_3(H_2O)]^-$ + $[(OH)(H_2O)]^-$		−40.83
$K_2Zn(OH)_4$	−3282.901091	−350.54

B. Binding Energies. The water and cation binding energies for the hydrated zincate complexes are given in Table 6. It can be seen that the stabilization of TZT due to hydration by two water molecules is greater than the stabilization of the dissociated $[Zn(OH)_3]^-$ and OH^- species by two waters. In addition, the very large binding energy for $K_2[Zn(OH)_4]$ suggests that this species is likely to be found in concentrated KOH solution. This has also been proposed in ref 14. While these gas-phase energies are far from definitive in identifying the preferred solvated structure(s) of $[Zn(OH)_4]^{2-}$ in concentrated KOH solutions, they, combined with the influence of water and cations on the geometry $[Zn(OH)_4]^{2-}$, point to the importance of condensed phase effects in determining stability of competing zincate species.

V. Oxodihydroxozincate

It has been proposed in the literature that $[ZnO(OH)_2]^{2-}$, or oxodihydroxozincate (ODHZ), could form in saturated or supersaturated zincate solutions by reaction 5, owing to a paucity of water molecules.[21] The most stable ODHZ species is the planar complex shown in Figure 3h, which is similar to the pinwheel structure of $[Zn(OH)_3]^-$. This complex has two Zn−O bonds of length 1.99 and 2.07 Å to the hydroxide ions (similar to TZT) and one shorter Zn−O bond of 1.81 Å. For comparison, the Re of ZnO is 1.71 Å at the same computational level. The O−Zn−O angle between OH− ligands is 94.3° and the Zn−O−H angles are 126.7 and 139.0°. The Zn EP charge is 0.82, similar to the charge in $[Zn(OH)_3]^-$. In our calculations, the proposed reaction for ODHZ formation from TZT (reaction 5) is endothermic by 52.7 kcal/mol in the absence of any hydration effects. However, compared to the total ligand binding energy of TZT and the hydration energy of Zn^{2+}, this is a rather small energy difference, indicating ODHZ is a viable zincate species for saturated solutions when the water molecules produced by the reaction (eq 5) would likely be engaged in solvating other ions or complexes.

VI. Conclusions

In this work we have presented the geometries and binding energies for the gas-phase $Zn(OH)^+$, $Zn(OH)_2$, $[Zn(OH)_3]^-$, and $[Zn(OH)_4]^{2-}$ zincate complexes. Our calculations reveal that $[Zn(OH)]^+$, $Zn(OH)_2$, and $[Zn(OH)_3]^-$ complexes are stable in

the gas phase; however, sequential binding energies reveal that TZT is unstable in the gas phase due to ligand−ligand repulsion and is likely to dissociate to $[Zn(OH)_3]^- + OH^-$. The hydroxide ligands exhibit dative bonding to the Zn atom and charge is transferred from the filled 1π orbitals of OH^- to the 4s orbital of Zn. The amount of charge donated is dependent upon the number of OH^- ligands and how close the ligands are to Zn. However, due to increasing Zn−O distance with increasing number of ligands, the Zn charge remains fairly constant at around 1 independent of the number of ligands. Based on these findings, and the extremely strong ligand binding energy in $[Zn(OH)]^-$, we believe $[Zn^{2+}(OH^-)_n]$ is not the best description of zincate species. Rather, these species are better considered as $[Zn^+(OH)-(OH^-)_{n-1}]$.

The Zn−O distance and O−Zn−O angles are determined largely by ligand−ligand repulsion and O···H attraction. Water was found to have relatively little influence on the geometry of the underlying $[Zn(OH)_n]^{2-n}$ complexes with the exception of $[Zn(OH)_4]^{2-}$. The TZT structure obtained in the gas phase is markedly different from that reported in experiments. The addition of two water molecules or two K^+ ions shortens the Zn−O bond lengths, bringing them more in line with what is seen in experiment, and the ZnO_4 subunit structure is nearly tetrahedral in these complexes, in agreement with experiment. Our calculations suggest that solvation effects are significant in determining the relative stabilities of various zincate complexes.

References and Notes

(1) Tuch, C. D. S. *Modern Battery Technology*; Ellis Horwood Limited: Chichester, England, 1991; p 79.
(2) Binder, L. O. In *Handbook of Battery Materials*; Benhard, J. O., Ed.; John Wiley and Sons: New York, 1999; p 195.
(3) www.duracell.com/Fun_Learning/index.html.
(4) Nishio, K.; Furukawa, N. In *Handbook of Battery Materials*; Benhard, J. O., Ed.; John Wiley and Sons: New York, 1999; p 19.
(5) Dirkse, T. P. *J. Electrochem. Soc.* **1954**, *101*, 328.
(6) Pinart, J.; Faucherre, J. *C. R. Acad. Sci. Ser. C* **1972**, *257*, 1149.
(7) Cain, K. J.; Melendres, C. A.; Maroni, V. A. *J. Electrochem. Soc.* **1987**, *134*, 519.
(8) Newman, G. H.; Blomgren, G. E. *J. Chem. Phys.* **1965**, *8*, 2744.
(9) van Doorne, W.; Dirkse, T. P. *J. Electrochem. Soc.* **1975**, *122*, 1.
(10) Debiemme-Chouvy, C.; Vedel, J.; Bellissent-Funel, M.; Cortes, R. *J. Electrochem. Soc.* **1995**, *142*, 1359.
(11) Briggs, A. G.; Hampson, N. A.; Marshall, A. *J. Chem. Soc., Faraday Trans. 2* **1974**, *70*, 1978.
(12) Fordyce, J. S.; Baum, R. L. *J. Chem. Phys.* **1965**, *43*, 843.
(13) *Zinc−Silver Oxide Batteries*; Fleisher, A., Lander, J. J., Eds.; John-Wiley and Sons: New York, 1971; p 29.
(14) Pandya, K. I.; Russell, A. E.; McBreen, J.; O'Grady, W. E. *J. Phys. Chem.* **1995**, *99*, 11967.
(15) Debiemme-Chouvy, C.; Vedel, J. *Extended Abstracts, Vol. 89-2*; Electrocehmical Society: Pennington, NJ, 1989; p 11, abstract 7.
(16) McBreen, J. In *The Science of Advanced Batteries*; Scherson, D. A., Ed.; Case Western Reserve University Press: Cleveland, OH, 1995.
(17) Dirkse, T. P. *J. Electrochem. Soc.* **1975**, *122*, 1.
(18) Dirkse, T. P. *J. Electrochem. Soc.* **1981**, *128*, 1412.
(19) Sharma, S. K.; Reed, M. *J. Inorg. Nucl. Chem.* **1976**, *38*, 1971.
(20) Dmitrenko, V. E.; Baolov, V. I.; Zubov, M. S.; Balyakina, N. N.; Kotov, A. V. *Electrokimiya* **1985**, *21*, 349.
(21) Bebiemme-Chouvy, C.; Vedel, J. *J. Electrochem. Soc.* **1991**, 138, 2538.
(22) Frisch, M. J.; Trucks, G. W.; Schlegel, H. B.; Scuseria, G. E.; Robb, M. A.; Cheeseman, J. R.; Zakrzewski, V. G.; Montgomery, J. A., Jr.; Stratmann, R. E.; Burant, J. C.; Dapprich, S.; Millam, J. M.; Daniels, A. D.; Kuden, K. N.; Strain, M. C.; Farkas, O.; Tomas, J.; Barone, V.; Cossi, M.; Cammi, R.; Menucci, B.; Pomelli, C.; Adamo, C.; Clifford, S.; Ochterski, J.; Petersson, G. A.; Ayala, P. Y.; Cui, Q.; Morokuma, K.; Malick, D. K.; Rabuck, A. D.; Raghavachari, K.; Foresman, J. B.; Cioslowski, J.; Ortiz, J. V.; Stefanov, B. B.; Liu, G.; Liashenko, A.; Piskorz, G.; Kormaromi, I.; Gomperts, R.; Martin, R. L.; Fox, D. J.; Keith, T.; Al-Laham, M. A.; Peng, C. Y.; Nanayakkara, A.; Gonzalez, C.; Challacombe, M.; Gill, P. M. W.; Johnson, B. G.; Chen, W.; Wong, M. W.; Andres, J. L.; Head-Gordon, M.; Replogle, E. S.; Pople, J. A. *GAUSSIAN 98 (Revision A.7)*; Gaussian, Inc.: Pittsburgh, PA, 1998.
(23) Dunning, T. H, Jr. *J. Chem. Phys.* **1989**, *90*, 1007.
(24) http://www.emsl.pnl.gov:2080/basisform.html.
(25) Lee, C.; Yang, W.; Parr, R. G. *Phys. Rev. B* **1988**, *37*, 785.
(26) Becke, A. D. *J. Chem. Phys.* **1993**, *98*, 5648.
(27) Dolg, M.; Wedig, U.; Stoll, H.; Preuss, H. *J. Chem. Phys.* **1987**, *86*, 866.
(28) Moore, C. E. 1949, 1952, 1971, Natl. Bur. Stand. Circ. No 467; USGPO: Washington, DC.
(29) $D_0(Zn-O) = 1.61$ eV was taken from guided ion-beam mass spectroscopy experiments of Clemmer, D. E.; Dalleska, N. F.; Armentrout, P. B. *J. Chem. Phys.* **1991**, *95*, 7263. $\omega_e(ZnO) = 805$ cm^{-1} was taken from photoelectron spectroscopy experiments Fancher, C. A.; de Clercq, H. L.; Thomas, O. C.; Robinson, D. W.; Bowen, K. H. *J. Chem. Phys.* **1998**, *109*, 8426.
(30) Bauschlicher, C. W., Jr.; Partridge, H. *J. Chem. Phys.* **1998**, *109*, 8430.
(31) Boldyrev, A. I.; Simons, J. *Mol. Phys.* **1997**, *92*, 365.
(32) Breneman, C. M.; Wiberg, K. B. *J. Comput. Chem.* **1990**, *11*, 361. Radii of 2.5 and 3.0 Å were used for Zn and K, respectively, and default Gaussian98 radii were used for H and O.
(33) Optimized coordinates for all zincate structures can be obtained at www.che.utah.edu/~gdsmith/tutorials/zmatrix.doc.